Lamination-Parameter-Based Mass Minimization of the Common Research Model Wing Using Sandwich Composites

Meddaikar, Yasser; Dillinger, J.K.S.; Silva, Gustavo H. C.; De Breuker, R.

DOI
10.2514/1.C037863

Licence
Dutch Copyright Act (Article 25fa)

Publication date
2025

Document Version
Final published version

Published in
Journal of Aircraft: devoted to aeronautical science and technology

Citation (APA)
Meddaikar, Y., Dillinger, J. K. S., Silva, G. H. C., & De Breuker, R. (2025). Lamination-Parameter-Based Mass Minimization of the Common Research Model Wing Using Sandwich Composites. *Journal of Aircraft: devoted to aeronautical science and technology*, *62*(6), 1605-1619. https://doi.org/10.2514/1.C037863

JOURNAL OF AIRCRAFT
Vol. 62, No. 6, November–December 2025

Lamination-Parameter-Based Mass Minimization of the Common Research Model Wing Using Sandwich Composites

Yasser M. Meddaikar* and Johannes K. S. Dillinger†
DLR, German Aerospace Center, 37073 Goettingen, Germany
Gustavo H. C. Silva‡
Boom Supersonic, Centennial, Colorado 80112
and
Roeland De Breuker§
Delft University of Technology, 2629 HS Delft, The Netherlands

https://doi.org/10.2514/1.C037863

Fiber-reinforced composites are widely used in primary aircraft structures on account of their superior performance when compared to metallic structures. When buckling is a dominant driver of the structural design, the use of sandwich composites could potentially yield more efficient designs. This paper applies a recently developed approach for optimizing practical commercial-scale aircraft wings using sandwich composites in a preliminary design stage to perform design studies using the NASA Common Research Model (CRM) as a reference. The approach uses lamination parameters as design variables in a continuous optimization step. Structural constraints for classic composite laminate design, such as material failure and buckling, and for sandwich design, such as crimping, wrinkling, dimpling, and core shear failure, are accounted for using industrial-standard and empirical methods driven by finite element analyses. The optimization studies present comparisons in structural weight between sandwich composite designs and their monolithic counterparts. The studies present several cases where sandwich composites offer superior structural performance, as well as potential cost savings by affording a lesser number of stringers in the design.

Nomenclature

$\boldsymbol{A}$	=	membrane stiffness matrix
$\boldsymbol{B}$	=	membrane-bending coupling matrix
b	=	stringer flange width
C_i	=	coefficients (empirical) for failure modes
$\boldsymbol{D}$	=	bending stiffness matrix
E	=	elastic modulus
$\boldsymbol{G}$	=	transverse shear stiffness matrix
G	=	Shear modulus
h	=	stringer height
$\boldsymbol{M}$	=	bending stress resultant
$\boldsymbol{N}$	=	in-plane stress resultant
$\boldsymbol{Q}$	=	transverse shear stress resultant
$Q_{[x,y]}$	=	transverse shear force
$S_{[L,W]z}$	=	transverse shear strength along L and W directions
s	=	cell size of honeycomb core
t	=	thickness
$\boldsymbol{U}$	=	lamina invariants
$\boldsymbol{x}$	=	design variables
γ	=	shear strain
ε	=	in-plane strain
θ	=	stacking angle distribution
ν	=	Poisson's ratio
$\xi^{[A,B_l,B_u,D]}_{\varsigma[1,2,3,4]}$	=	lamination parameters
σ	=	in-plane stress
τ	=	shear stress
$\bullet_f$	=	property of facesheet
$\bullet_c$	=	property of core

Received 31 December 2023; accepted for publication 23 March 2025; published online Open Access 31 July 2025.

*Research Scientist, Loads and Aeroelastic Design, Institute of Aeroelasticity; muhammad.meddaikar@DLR.de (Corresponding Author).
†Research Scientist, Loads and Aeroelastic Design, 12876, E Adam Aircraft Cir.
‡Senior Structural Engineer, Institute of Aeroelasticity.
§Associate Professor, Faculty of Aerospace Engineering—Aerospace Structures and Materials.

I. Introduction

OVER the last few decades, the aerospace industry has seen a steady increase in the use of composite materials [1]. The superior mechanical properties of composites, ability to tailor their stiffness properties, and possible lower manufacturing costs due to integration of parts have been some of the reasons for the increased focus on their research and application.

In today's commercial aircraft, monolithic laminates have been predominantly used where load-carrying wing-box structures have been concerned, while sandwich composites have been restricted to secondary substructures such as fairings, ailerons, flaps, and rudders. Monolithic composites here refer to composite laminates comprising a single material basis, for instance, a carbon fiber and epoxy system, while sandwich composites referred to here comprise two facesheets made up of a laminate such as a carbon/epoxy system separated by core material of low density such as honeycomb. An example of such a sandwich composite construction containing facesheets of equal thickness is shown in Fig. 1. In applications such as wind turbines, sailplanes, or satellites, sandwich composites have also been used in primary structures with several optimization approaches investigated, for instance, in [2–7]. Practical experience shows that the benefits of sandwich composites come alongside a number of unique engineering challenges, which must be carefully considered in realistic designs: damage tolerance and its characterization, manufacturing complexities at joints and ramp-downs, and complex identification and carrying out of repairs, to name a few [8]. Ongoing research in several university and research groups aims to tackle these very challenges on account of the potential benefits of sandwich composites [3,8–13].

The present trend of aircraft wings shows designs that are dominated by stiffness requirements when compared to strength requirements [14–17], especially in the upper skin. That is, buckling stability drives the structural design in these regions. Moreover, outer sections of the wing are sized due to minimum gauge requirements arising out

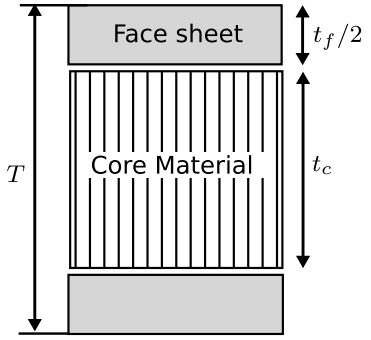

Fig. 1 Cross-section of a classic sandwich composite (t_f = facesheet thickness, t_c = core thickness, T = total thickness).

of handling and manufacturing needs. With advancements in materials beyond carbon fiber T300 and IM7 to today's state-of-the-art materials such as the high-strength T1100G and IM10 [18], designers can only expect strength requirements to be further overshadowed by stiffness and handling requirements. In such cases, sandwich composites could prove to be an interesting solution in being able to efficiently handle buckling stability. As future materials evolve with properties heading toward carbon nanotubes, hypothetically speaking, sandwich composites could once again be one efficient solution in meeting both buckling and manufacturing needs. The increase in specific bending stiffness of sandwich composites enables not only the design of lighter panels but also a reduction of global stiffener-reinforcers whose primary purpose is to inhibit structural buckling, further increasing the potential weight savings and lowering manufacturing costs.

The potential benefits and challenges of sandwich composites in aerospace applications have motivated a wide range of research covering topics such as characterization of failure modes [19–21], development of modeling strategies [22,23], and optimization of sandwich composites [2,4–6,24–41]. Some of the relevant literature pertaining to aerospace applications in the latter is discussed further.

Miki et al. [25] define a modified set of lamination parameters specific to sandwich composites, using the approach to make graphical studies on the Miki diagram. Balabanov et al. [30] and Weckner et al. [32] optimize an in-plane loaded sandwich panel using classical lamination parameters subjected to strength and stability constraints. Schmit et al. [24] present an optimization of a rectangular wing box with sandwich composites using a multilevel optimization strategy. The approach is based on orthotropic linear stress rectangular (OLSR) elements together with predefined laminate angles. The approach presents a valid strategy for conceptually optimizing sandwich composites but is restrictive in its general applicability. Jin et al. [33] apply lamination parameters to the design of composite sandwich panels with aeroelastic constraints. Lamination parameters of the facesheets and transverse shear modulus of the core are used as design variables in a weight minimization problem subjected to flutter and divergence speed constraints. Moors et al. [38] study different design concepts, including sandwich composites, in the design of a composite wing box using a conceptual design tool based on analytical and semi-empirical approaches. Yuan et al. [29] present the optimization of sandwich panels for fuselage applications. An analytical solution for facesheet wrinkling and structural buckling is introduced, while the optimal weight of the sandwich composite is obtained using a multistep sequential approach. Fan et al. [37] optimize a multipanel sandwich composite structure subjected to buckling and strength constraints. A genetic algorithm (GA) is proposed to optimize for the facesheet layup together with analytical solutions for buckling and strength. Irisarri et al. [40] propose a strategy to optimize sandwich composites using a three-step approach: a gradient-based optimization in the first step using lamination parameters, an evolutionary algorithm in the second step to obtain the facesheet laminates, and a third optimization step to overcome infeasibilities in the design arising out of the stiffness variations between the first and second steps. The approach is applied to the design of a generic dual-launch spacecraft system. Seyyedrahmani et al. [42] present an approach to optimize sandwich panels considering different simultaneous objective functions, such as maximizing buckling load, maximizing fundamental natural frequency or natural frequency gap, and minimizing cost to arrive at Pareto-optimal solutions. The approach is based on a spectral Chebyshev formulation using a first-order shear deformation theory (FSDT). Sandwich composites for wing-box applications have been investigated mainly within research programs such as the bismaleimide (BMI) wing box [43] by Northrop Grumman and the National Aeronautics and Space Administration (NASA). The most famous industrial application of sandwich composite to the primary wing box is perhaps on the Beechcraft Starship, which was manufactured in the 1980s and 1990s. Another study of interest is the Advanced Technology Composite Aircraft Structures (ATCAS) [44,45] program by Boeing in the 1990s, investigating potential composite technologies for fuselage designs. A skin-stringer frame and a sandwich configuration were studied with in-depth considerations on the impact on manufacturing and lifetime costs on different fuselage panels.

A review of the above literature shows that practical studies addressing performance comparisons between traditional monolithic composite designs and sandwich composites for realistic, large-scale, commercial-type wings have not been considered in the past. More recently, the authors presented a first step in this direction [46] by studying weight comparisons between sandwich and monolithic composites at the level of skin panels, using the CRM as a benchmark wing. A lamination-parameter-based approach for the stiffness optimization considering material failure through angle minus laminate (AML) [47], buckling instability, facesheet wrinkling, shear crimping, facesheet dimpling, and core-shear failure is applied. The results showed that, depending on the spanwise section considered, skin panels with sandwich composite design exhibit significant weight savings when compared to classic monolithic composite design. The study also showed that for lightly loaded regions near the wing-tip, a larger stringer pitch can be afforded at low penalties to structural weight. The present work aims to further this by performing optimization studies on the CRM wing representative of a preliminary stage of design in order to arrive at weight comparisons between today's monolithic composites and potentially beneficial sandwich composites.

For the structural optimization studies in this paper, the NASA Common Research Model (CRM) [48] is chosen, more specifically a structural model of the CRM wing generated at the German Aerospace Center (DLR)–Institute of Aeroelasticity, under the configuration name FERMAT [49]. The CRM has been used as a benchmark case for several studies, including some of the more recent works [50–54]. For instance, the topology optimization of the stiffeners of the wing box [51] and aerostructural design of the CRM wing box using different design technologies such as conventional carbon-fiber-reinforced composite and tow-steered carbon-fiber-reinforced composite [53] both show buckling constraints on the wing box to be active, furthering one of the primary motivations for the present work.

The rest of this paper is organized as follows: Section II summarizes the design methodology followed in the optimization study, followed by a discussion on the treatment of design variables in the case of monolithic and sandwich composites in Sec. III. The CRM wing, which is the application considered, is presented in Sec. IV, and a summary of the optimization objective and constraints in Sec. V. The results from the optimization study are discussed in Sec. VI, followed by a conclusion and outlook based on the presented work.

II. Design Methodology

The optimization strategy used in this paper can be split into two core components: i) the structural constraints that define the feasibility of a design and ii) the lamination parameters as design variables and their associated constraints, which are used to define

the optimization problem. Details on the approach have been presented in [46] and are summarized in the present section for completeness.

A. Structural Constraints for Sandwich Composite Design

The failure modes in sandwich composites for typical wing-box-type structures as discussed in the Composite Materials Handbook-17 (CMH-17) [55] are shown in Fig. 2.

The first two failure modes, namely material failure and buckling, are typically considered in the preliminary design stage for monolithic composites. The additional failure modes—wrinkling, core shear failure, crimping, and dimpling—need to be accounted for when designing with sandwich composites. In the case of stringers, only material failure and stringer crippling [56] are included as constraints. The failure modes are accounted for using different approaches, driven by finite element (FE) analysis, and are summarized in Table 1.

In Eqs. (2–7), the geometric quantities t_c, t_f, h, and s are the thickness of the core, thickness of each facesheet, the distance between the midplanes of the upper and lower facesheets, and the cell size of the honeycomb core, respectively. For composite facesheets, the stiffness terms are direction-dependent—E_f represents the effective bending stiffness of the facesheet in the direction of loading and is

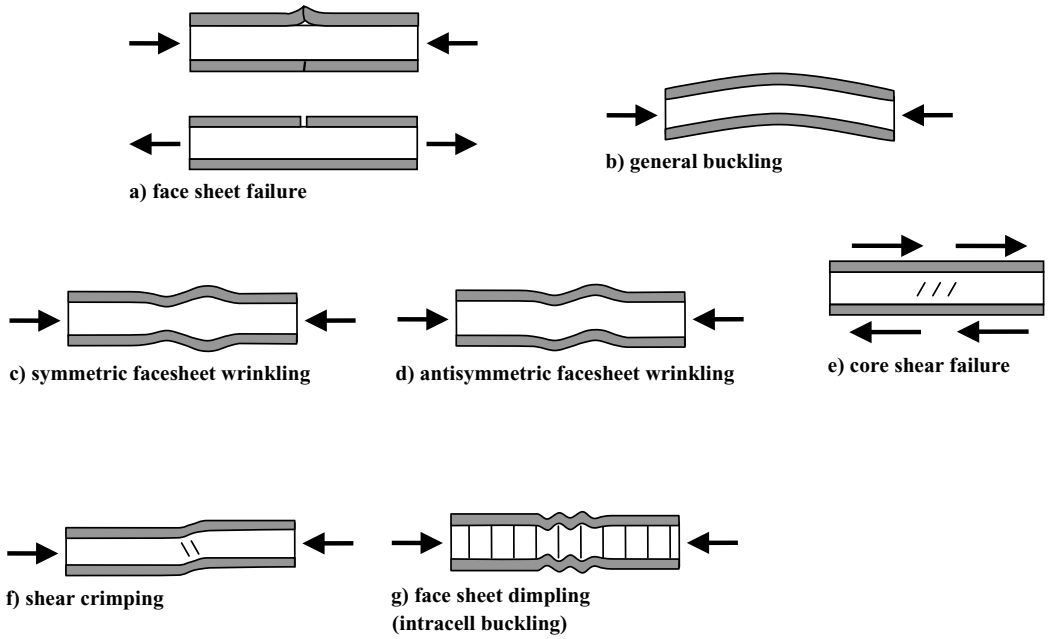

Fig. 2 Failure modes of sandwich composites [55].

Table 1 Structural constraints included in the optimization

Failure mode	Method	
Strain failure	Angle minus laminate (AML) [47]	
	$\epsilon_{\min} < \epsilon < \epsilon_{\max}$ (stringers)	(1)
Stringer crippling [56]	$\sigma_{\text{crip}} = \sigma_c^u \dfrac{1.63}{\left(\dfrac{b}{h}\right)^{0.717}}(1)$	(2)
Buckling	Linear buckling solver in MSC.NASTRAN	
Wrinkling [55]		
	if $t_c \geq 1.82 t_f \sqrt[3]{\dfrac{E_f E_c}{G_c^2}}$, $\sigma_{\text{wrink}} = C_1 (E_f E_c G_c)^{1/3} + C_2 G_c \dfrac{t_c}{t_f}$	(3)
— —	if $t_c \leq 1.82 t_f \sqrt[3]{\dfrac{E_f E_c}{G_c^2}}$, $\sigma_{\text{wrink}} = C_3 \sqrt{\dfrac{t_f}{t_c} E_c E_f} + C_4 G_c \dfrac{t_c}{t_f}$	(4)
Shear crimping [55]	$\sigma_{\text{crimp}} = \dfrac{h^2 G_c}{(2t_f) t_c}$	(5)
Facesheet dimpling [55]	$\sigma_{\text{dimp}} = \dfrac{1}{t_f} \left(\dfrac{\pi}{s}\right)^2 \{D_{11} + 2(D_{12} + 2D_{66}) + D_{22}\}$	(6)
Core shear failure [55]	$\tau_{xz} = \dfrac{Q_x}{t_c}, \qquad \tau_{yz} = \dfrac{Q_y}{t_c}$	(7)

calculated from the bending stiffness matrix $\boldsymbol{D}$. E_c is the core elastic modulus normal to the sandwich facesheets, and G_c is the core shear modulus. Honeycomb cores tend to have different properties in their ribbon and transverse directions; as a result, the values G_{xz}, G_{yz}, and $\sqrt{G_{xz}G_{yz}}$ are suggested in the CMH-17 to be used in place of G_c, depending on whether the loading is in the *X*, *Y*, or *XY* direction. The coefficients C_1–C_4, in the case of wrinkling in Eqs. (3) and (4), are generally adapted to experimental results, and a wide range of values have been reported, for instance, [56–58]. Conservative values of $C_1 = 0.247$, $C_2 = 0.078$, $C_3 = 0.33$, and $C_4 = 0$ are suggested in the CMH-17. The failure stresses for the above sandwich failure modes are defined for a uniaxial state of compression. Loading states along different directions can be considered by using corresponding values for the directional stiffnesses. The transverse loads Q_x and Q_y are extracted as forces from a static analysis in MSC.NASTRAN. In Eq. (2), b and h are the flange width and height of the *T*-stringer, and σ_c^u is the ultimate compressible strength of the material.

For the sake of convenience, the failure stresses in the case of wrinkling, crimping, and dimpling are recast as failure strains through the directional in-plane stiffness. In the following sections, the failure criteria of AML, crippling, wrinkling, crimping, and dimpling are collectively denoted as strain-based failure criteria, while core shear failure is termed a "force-based failure criterion." Correspondingly, the terms "strain failure index" and "force failure index" are used when aggregating these sets of failure modes.

B. Lamination-Parameter-Based Continuous Optimization

The composite optimization problem is solved using a commonly applied two-step approach [15,59–65]. In the first step, lamination parameters and thickness of the composite are used as design variables using efficient gradient-based optimizers. In the second step, the optimum stiffness design obtained earlier is used as a starting point to obtain an optimal stacking sequence distribution, for instance, in [15,65–67].

The continuous optimization step is the focus of this paper, targeting design studies representative of a preliminary design stage. The result obtained from this step yields the optimal stiffness distribution of the structure and is indicative of the structural performance attainable.

The optimization problem can be stated as follows:

$$\begin{aligned} \min_{\boldsymbol{x}} \quad & f(\boldsymbol{x}) \\ \text{subject to:} \quad & P_j(\boldsymbol{x}) \le 1, \quad j = 1 \ldots n_p \\ & C_k(\boldsymbol{x}) \le 1 \quad k = 1 \ldots n_c \\ & x_i^l \le x_i \le x_i^u \quad x_i \in \boldsymbol{x} \end{aligned} \tag{8}$$

The design variables $\boldsymbol{x}$ comprise thickness and lamination parameters. The objective function $f(\boldsymbol{x})$ is to be minimized, structural weight in this case. The physical constraints *P*, which are the failure modes, and the admissibility constraints *C* on the design variables are normalized such that values less than 1 are feasible.

The lamination parameter scheme presented in [39] is applied for the design of sandwich composites. This is an extension to the classical lamination parameters [68,69] defined for laminates having a single material basis.

In the general case of symmetric sandwich composites, where both facesheet and core comprise anisotropic composite materials, the exact in-plane and bending stiffness matrices are calculated as

$$\boldsymbol{A} = t_c[\boldsymbol{\xi}^A]_c\{\boldsymbol{U}\}_c + t_f[\boldsymbol{\xi}^A]_f\{\boldsymbol{U}\}_f \tag{9}$$

$$\boldsymbol{D} = \frac{t_c^3}{12}[\boldsymbol{\xi}^D]_c\{\boldsymbol{U}\}_c + \frac{t_f^3}{12}[\boldsymbol{\xi}^D]_f\{\boldsymbol{U}\}_f + \frac{t_c t_f}{4}(t_f[\boldsymbol{\xi}^{B_u}]_f + t_c[\boldsymbol{\xi}^A]_f)\{\boldsymbol{U}\}_f \tag{10}$$

where t is the thickness, $\boldsymbol{U}$ is the matrix of laminate invariants, $\boldsymbol{\xi}^{A,B_u,D}$ are lamination parameters, and subscripts f and c denote properties for the facesheet and core, respectively. The lamination parameters in the above equations are defined as

$$\xi^A_{[1,2,3,4]} = \frac{1}{2}\int_{-1}^{1}[\cos 2\theta(\bar{z}), \cos 4\theta(\bar{z}), \sin 2\theta(\bar{z}), \sin 4\theta(\bar{z})]\,\mathrm{d}\bar{z} \tag{11}$$

$$\xi^{B_u}_{[1,2,3,4]} = -2\int_{-1}^{0}[\cos 2\theta(\bar{z}), \cos 4\theta(\bar{z}), \sin 2\theta(\bar{z}), \sin 4\theta(\bar{z})]\bar{z}\,\mathrm{d}\bar{z} \tag{12}$$

$$\xi^{B_l}_{[1,2,3,4]} = 2\int_{0}^{1}[\cos 2\theta(\bar{z}), \cos 4\theta(\bar{z}), \sin 2\theta(\bar{z}), \sin 4\theta(\bar{z})]\bar{z}\,\mathrm{d}\bar{z} \tag{13}$$

$$\xi^D_{[1,2,3,4]} = \frac{3}{2}\int_{-1}^{1}[\cos 2\theta(\bar{z}), \cos 4\theta(\bar{z}), \sin 2\theta(\bar{z}), \sin 4\theta(\bar{z})]\bar{z}^2\,\mathrm{d}\bar{z} \tag{14}$$

The definition of the $\boldsymbol{\xi}^{B_l}$ is presented here for the sake of completeness. For a symmetric sandwich composite, such as when a core material is inserted into a symmetric monolithic laminate split at the center, $\boldsymbol{\xi}^{B_l} = -\boldsymbol{\xi}^{B_u}$. Since the present study considers such symmetric sandwich composites, the $\boldsymbol{\xi}^{B_l}$ terms are simplified in Eq. (10) through $\boldsymbol{\xi}^{B_u}$. While the sandwich composites in this study are considered to be symmetric, the individual facesheets need not be symmetric but are certainly antisymmetric to each other. The lamination parameters and the material invariants can be expressed in vectorial form as

$$[\boldsymbol{\xi}] = \begin{bmatrix} 1 & \xi_1 & \xi_2 & 0 & 0 \\ 1 & -\xi_1 & \xi_2 & 0 & 0 \\ 0 & 0 & -\xi_2 & 1 & 0 \\ 0 & 0 & -\xi_2 & 0 & 1 \\ 0 & \xi_3/2 & \xi_4 & 0 & 0 \\ 0 & \xi_3/2 & -\xi_4 & 0 & 0 \end{bmatrix} \tag{15}$$

$$\begin{Bmatrix} U_1 \\ U_2 \\ U_3 \\ U_4 \\ U_5 \end{Bmatrix} = \frac{1}{8}\begin{bmatrix} 3 & 3 & 2 & 4 \\ 4 & -4 & 0 & 0 \\ 1 & 1 & -2 & -4 \\ 1 & 1 & 6 & -4 \\ 1 & 1 & -2 & 4 \end{bmatrix}\begin{Bmatrix} Q_{11} \\ Q_{22} \\ Q_{12} \\ Q_{66} \end{Bmatrix} \tag{16}$$

The full set of design variables for an optimization in this general case is

$$\boldsymbol{x} = \left\{ t_c \mid \quad t_f \mid \quad \boldsymbol{\xi}_c^A \mid \quad \boldsymbol{\xi}_f^A \mid \quad \boldsymbol{\xi}_f^{B_u} \mid \quad \boldsymbol{\xi}_c^D \mid \quad \boldsymbol{\xi}_f^D \right\}^T \tag{17}$$

For sandwich composites containing an isotropic core material with a low stiffness in comparison with the facesheet material, such as for foam or honeycomb cores, the terms involving the stiffness contributions from the core in Eqs. (9) and (10) can be neglected. The stiffness matrices can be expressed as

$$\boldsymbol{A} = t_f[\boldsymbol{\xi}^A]_f\{\boldsymbol{U}\}_f \tag{18}$$

$$\boldsymbol{D} = \frac{t_f^3}{12}[\boldsymbol{\xi}^D]_f\{\boldsymbol{U}\}_f + \frac{t_c t_f}{4}(t_f[\boldsymbol{\xi}^{B_u}]_f + t_c[\boldsymbol{\xi}^A]_f)\{\boldsymbol{U}\}_f \tag{19}$$

resulting in a reduced set of design variables:

$$\boldsymbol{x} = \left\{ t_c \mid \quad t_f \mid \quad \boldsymbol{\xi}_f^A \mid \quad \boldsymbol{\xi}_f^{B_u} \mid \quad \boldsymbol{\xi}_f^D \right\}^T \tag{20}$$

In the case of monolithic composites, the second term in Eq. (19) is zero, with $t_c = 0$, resulting in the definitions of $\boldsymbol{A}$ and $\boldsymbol{D}$ matrices corresponding to the classical lamination parameters. Approximations for $\boldsymbol{D}$ for sandwich composites that circumvent the definition of the $\boldsymbol{\xi}_f^{B_u}$ lamination parameters are discussed in [39].

1. Accounting for Transverse Shear Stiffness

The transverse shear stiffness in the case of sandwich composites is considered using the Reissner–Mindlin plate theory.

The laminate constitutive relation can be represented as

$$\begin{Bmatrix} \boldsymbol{N} \\ \boldsymbol{M} \\ \boldsymbol{Q} \end{Bmatrix} = \begin{bmatrix} \boldsymbol{A} & \boldsymbol{B} & 0 \\ \boldsymbol{B} & \boldsymbol{D} & 0 \\ 0 & 0 & \boldsymbol{G} \end{bmatrix} \tag{21}$$

where $\boldsymbol{N}$, $\boldsymbol{M}$, and $\boldsymbol{Q}$ are the in-plane, bending, and transverse shear stress resultants, respectively.

The transverse shear component of the laminate constitutive relation is defined by the stress resultant

$$\boldsymbol{Q} = \int_{-T/2}^{T/2} \begin{Bmatrix} \tau_{yz} \\ \tau_{xz} \end{Bmatrix} = \begin{Bmatrix} Q_y \\ Q_x \end{Bmatrix} \tag{22}$$

and the stiffness terms

$$\boldsymbol{G} = \begin{bmatrix} G_{44} & G_{45} \\ G_{45} & G_{55} \end{bmatrix} \tag{23}$$

The individual terms in the stiffness matrix are obtained by integrating through the thickness under the assumption that each kth ply in the N-ply laminate has a constant thickness and laminate orientation, resulting in the stiffness terms

$$G_{ij} = \sum_{k=1}^{N} (z_k - z_{k-1}) \bar{Q}_{ij}^k \tag{24}$$

The thickness-dependent term observed in the above equation $\sum_{k=1}^{N} (z_k - z_{k-1})$ is analogous to the in-plane stiffness matrix $\boldsymbol{A}$. Consequently, the transverse shear stiffness matrix can be expressed in terms of existing in-plane lamination parameters and through material invariants as presented in [30] as

$$\{\hat{\boldsymbol{G}}\} = \begin{bmatrix} 1 & \xi_1^A \\ 0 & -\xi_3^A \\ 1 & -\xi_1^A \end{bmatrix} \begin{Bmatrix} U_6 \\ U_7 \end{Bmatrix} \tag{25}$$

$$\{\boldsymbol{G}\} = [T]\{\hat{G}\} \tag{26}$$

in a vectorized form, where $\hat{\boldsymbol{G}}$ is the thickness-normalized transverse shear stiffness matrix and T is the total thickness.

The material invariants are defined as

$$\begin{Bmatrix} U_6 \\ U_7 \end{Bmatrix} = \frac{1}{2} \begin{bmatrix} 1 & 1 \\ 1 & -1 \end{bmatrix} \begin{Bmatrix} Q_{44} \\ Q_{55} \end{Bmatrix} \tag{27}$$

where Q_{44} and Q_{55} are a part of the transverse shear terms in the stress–strain relationship for a transversely isotropic lamina with values being the engineering constants G_{23} and G_{13}, respectively.

$$\begin{Bmatrix} \tau_{23} \\ \tau_{13} \end{Bmatrix} = \begin{bmatrix} Q_{44} & 0 \\ 0 & Q_{55} \end{bmatrix} \begin{Bmatrix} \gamma_{23} \\ \gamma_{13} \end{Bmatrix} \tag{28}$$

It is to be noted that MSC.NASTRAN can account for transverse shear correction factors that depend on the stacking sequence of the laminate as well. This correction factor is not considered here given that the optimization is performed in the lamination parameter space. This correction can be considered when working directly with the final stacking sequence of the composite laminates or by accounting for using appropriate submodeling techniques [40].

2. Admissibility Constraints

Admissibility constraints for lamination parameters are chosen as formulated in [70] as

$$\begin{aligned} &\text{Bounds}: -1 \le \xi_{[1,2,3,4]}^{[A,B_u,D]} \le 1 \\ &\text{Feasibility}: \text{For } k = A, B_u, D, \\ &\qquad 2(\xi_1^k)^2 - 1 \le \xi_2^k \le 1\text{–}2(\xi_3^k)^2 \\ &\qquad 2(\xi_2^k + 1)(\xi_3^k)^2 - 4\xi_1^k \xi_3^k \xi_4^k + (\xi_4^k)^2 \\ &\qquad \le [\xi_2^k - 2(\xi_1^k)^2 + 1](1 - \xi_2^k) \end{aligned} \tag{29}$$

More extensive formulations of these constraints exist in the literature [71–74]; however, the above form has been utilized on account of its simplicity and the acceptable results attainable [15] in retrieving the stacking sequence in the second step.

For practical design requirements such as the use of standard angles $[0°, \pm 45°, 90°]$, requirements on balanced laminates and limits on angle fractions (such as the 10% rule, which is commonly applied to avoid matrix-dominated behavior) can be formulated on the lamination parameters as

$$\text{Standard Angles}: \xi_4^{[A,B_u,D]} = 0 \tag{30}$$

$$\text{Balance}: \xi_3^A = 0 \tag{31}$$

$$\begin{aligned} &\text{Angle Fraction}: v_0 = \frac{\xi_2^A + 2\xi_1^A + 1}{4}, \quad v_{90} = \frac{\xi_2^A - 2\xi_1^A + 1}{4}, \\ &v_{\pm 45} = \frac{\pm 2\xi_3^A - \xi_2^A + 1}{4} \end{aligned} \tag{32}$$

Further constraints on the lamination parameters, such as those due to blending [75], can also be included but have not been considered in this work.

III. Monolithic and Sandwich Design Variables in Optimization

When considering monolithic and sandwich composites as two design options, the selection between them will be driven by their relative performance. An optimal solution might include both design options in different regions of the wing or aircraft, given that particular design loads might favor one design over the other. Having an optimization scheme that enables a smooth transition or selection between a monolithic and a sandwich design would enable this automated selection. One way to enable this within a continuous optimization setup is by modeling the sandwich failure constraints such that the constraints become active only when a core thickness is added. In other words, there is a positive gradient of the failure index with respect to the core thickness.

This is seen in the case of the wrinkling constraint shown in the failure map in Fig. 3. The failure indices of different sandwich failure modes are plotted for varying core thickness on one element close to the wing midspan as an example while keeping the element loads constant. The element considered is in the upper skin, with the wing box subjected to a pull-up maneuver as an example, and

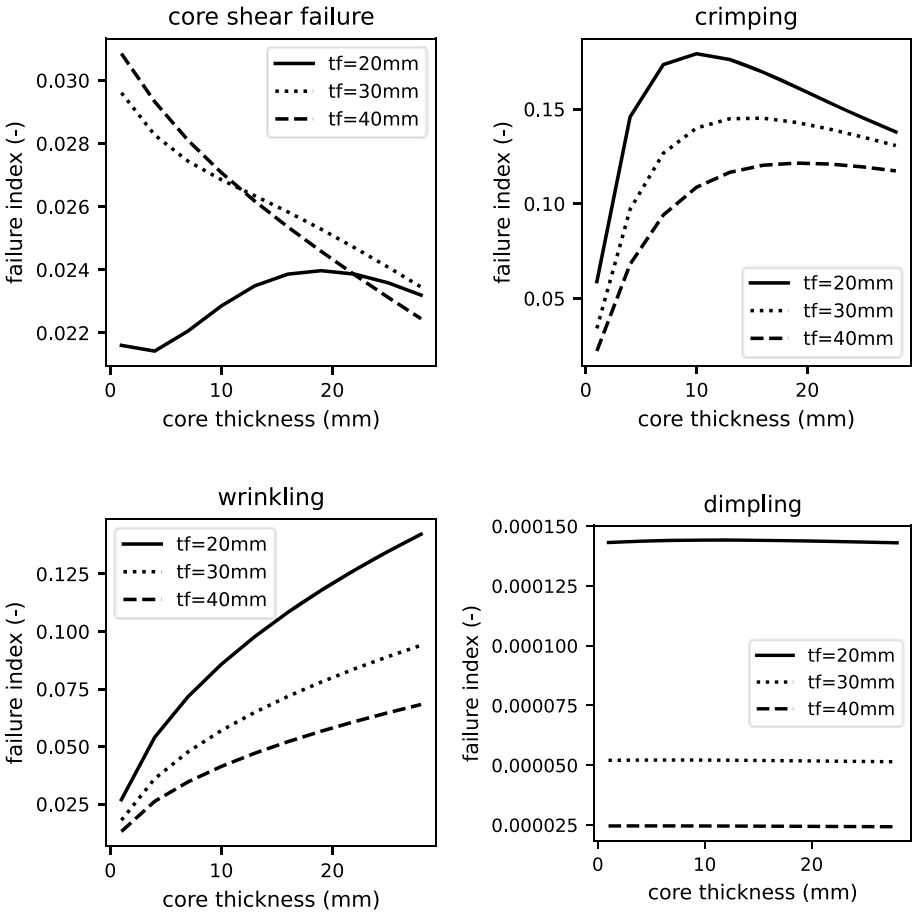

Fig. 3 Failure index for different sandwich failure modes in element 64,100,968 (near wing midspan).

experiences a predominantly compressive load with the following strain state $\epsilon_x = -4098\mu\epsilon$, $\epsilon_y = 1333\mu\epsilon$, $\gamma_{xy} = 460\mu\epsilon$. In this case, the thickness of the facesheet and core are varied for a selected set of lamination parameters, $\xi^A_{1-4} = \xi^B_{1-4} = \xi^D_{1-4} = 0$, that is, a quasi-isotropic or "black aluminum" laminate. A normalized failure index is chosen such that a value greater than 1 denotes failure. In the case of an optimization problem including only the wrinkling constraint, a continuous optimizer will tend to add core material where beneficial and tend toward reducing core thickness when detrimental. By including a suitable minimum core thickness in a postprocessing step, the optimal design variables can be interpreted as monolithic or sandwich design regions.

This, however, is not the case when considering other failure modes. In the case of core shear failure, for instance, the gradient of the failure index with respect to the core thickness points toward increasing core thickness to alleviate the failure mode, whereas reducing the core thickness to 0 mm, that is, to a monolithic laminate, should result in the failure mode itself ceasing to exist. The behavior changes drastically for different facesheet thicknesses as well. An easier example is the dimpling constraint that does not explicitly depend on the core thickness, as seen in Eq. (6). The core thickness only plays a role in the load redistribution arising out of a changed $\boldsymbol{D}$ matrix on account of the core. In both cases, the constraint is effectively a step function at zero core thickness, making it difficult to handle in a gradient-based optimization environment.

In order to enable an automatic switch between monolithic and sandwich composites, a mixed continuous-discrete handling of design variables and constraints is needed. In the present work, the choice between monolithic and sandwich composite design for a given region is made beforehand, and the optimizer works only with the design variables and constraints that have been set up in the initial optimization problem.

IV. Model Description

The structural optimization studies in this paper are performed on the NASA CRM wing [48], specifically on a structural model of the CRM wing generated at the DLR—Institute of Aeroelasticity [49], under the configuration name FERMAT shown in Figs. 4 and 5. The structural model comprises shell and beam elements, with homogenized membrane, bending, and transverse shear stiffness terms for the shell elements in the skin.

The wing model is optimized for two static maneuver points identified as critical in the flight envelope based on a preliminary downselection. These are listed in Table 2 and elaborated in [49]. The maximum takeoff weight (MTOW) of the configuration corresponds to 260,000 kg.

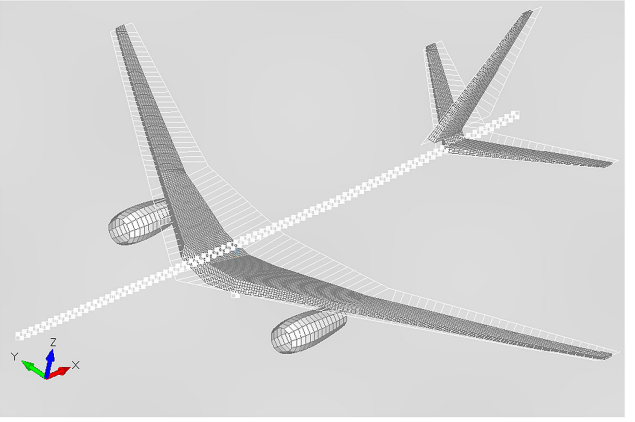

Fig. 4 Structural FE model of the CRM aircraft (FERMAT configuration).

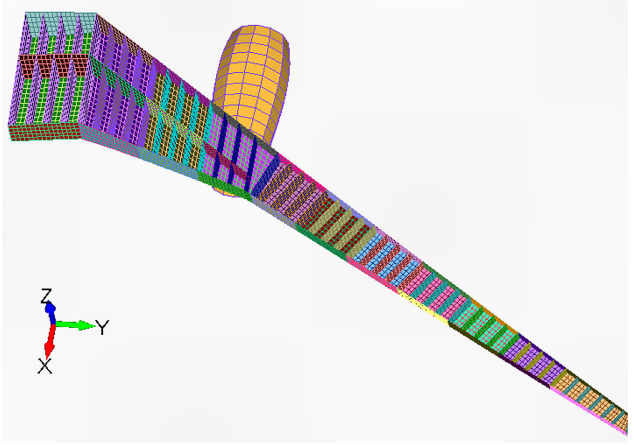

Fig. 5 Structural FE model of the CRM wing (without upper skin for visualization).

Table 2 Static maneuver load cases considered in the optimization (EAS, equivalent air speed)

Mass case	EAS, m/s	n_z, g	Ma	Flight altitude, m	$\bar{q}$, Pa
MTOW	192.4	+2.5	0.567	0	22,795
MTOW	221.2	−1.0	0.99	6,523	30,111

A. Material Properties

For the monolithic laminates and facesheets in the sandwich composite, a carbon fiber epoxy composite (IM7/8552) with the material properties listed in Table 3 is used.

Material failure in the composite laminate is accounted for using the AML approach. Failure strengths in compression from experiments for different values of AML [76] are shown in Fig. 6. The three curves represent open-hole (OHC), filled-hole (FHC), and unnotched (UNC) levels of damage under compression.

Table 3 Material properties of carbon-epoxy facesheets (Hexcel IM7/8552 UD)

Parameter	Value
Density, kg/m^3	1580
E_1, GPa	147.8
E_2, GPa	10.3
G_{12}, GPa	5.9
ν_{12}	0.27

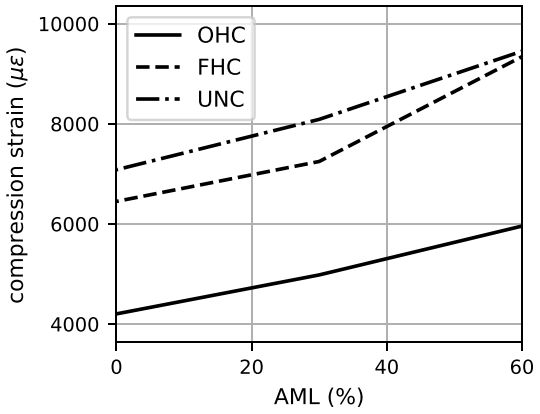

Fig. 6 Variation of allowable strains with AML for IM7/8552 composite [76].

In the present study, two types of honeycomb materials for the sandwich core are studied: 5052 Aluminum and HRH10 Nomex (aramid). The in-plane stiffness parameters E_1, E_2, and G_{12} of the honeycomb are nominally set close to zero ($E_1 = E_2 = 0.1$, $G_{12} = 0.039$) since they are not expected to carry in-plane loads. The other relevant properties [77] are listed in Table 4. The properties of the honeycomb material are anisotropic in nature, arising from the different characteristics along the direction of the ribbon (denoted by subscript L) and transverse to the ribbon direction (denoted by subscript W). The principal material axis for both the facesheet and the core is oriented along the front spar, such that directions 1 (in the composite 1–2 orientation system) and L (in the core L–W orientation system) are along this material axis for the facesheet and core material, respectively.

B. Buckling Constraint and Mesh Fineness

The optimization problem is set up with two parallel models: i) a global finite element (GFEM) or dynamic type model for strains (such as one shown in Fig. 5) and ii) a finer mesh FE model for global buckling using the SOL105 [78] solver in MSC.NASTRAN. The rationale behind using models with different meshes is that for the global-level structural optimization, which is the aim of this work, a mesh that is suitable for a loads analysis is typically utilized, as in this study as well. However, this mesh is not sufficient to capture inter-stringer or inter-rib stiffener modes, which is why a finer mesh is used for the buckling analysis.

For the buckling model, a first mesh convergence study is performed and shown in Table 5. M0 denotes the GFEM-type model having one element in the chord direction between two stiffeners and four elements in the spanwise direction between two ribs. Meshes M2–M4 are set up by splitting each element from M0 into two, three, and four elements, respectively, as shown in Fig. 7. Table 5 shows, for instance, that the model denoted as M1 shows a good compromise between accuracy and computation time. Such a mesh convergence study could be misleading, given that the critical buckling factors are dependent on the stiffness of the model being considered, and different modes might become critical that are possibly not captured by coarser models.

This is evident when using the models M1–M4 for the buckling analysis in an optimization. The optimized mass varies widely, and the buckling factor that drove the actual design itself is larger than 1.5 and hence deemed safe by the optimizer. The optimal design when evaluated with the finest mesh M4 shows largely violating buckling factors, given that more localized modes, between two stringers for instance, are captured by the fine M4 model. A sufficiently fine mesh, M4 in this case, would involve impractically large run times. The optimization is elaborated later in Sec. V, but the

Table 4 Material properties of honeycomb core material [77]

Density, kg/m^3	Cell size, mm	E_z, MPa	G_{Lz}, MPa	S_{Lz}, MPa	G_{Wz}, MPa	S_{Wz}, MPa
Hexcel HRH10 Nomex (aramid)						
64	3	190.0	63.0	2.0	35.0	1.0
5052 Aluminium						
144	3	1,034.0	483.0	2.3	214.0	1.5

Table 5 Mesh convergence of CRM model for buckling solution in MSC.NASTRAN (critical buckling factor greater than 1.5 denotes feasible design)

Model	Critical buckling factors	No. of elements	Computation time, s
M0	4.17, 5.23	∼22 k	93
M1	3.95, 4.64	∼62 k	451
M2	3.94, 4.47	∼120 k	1135
M4	3.94, 4.43	∼195 k	4671

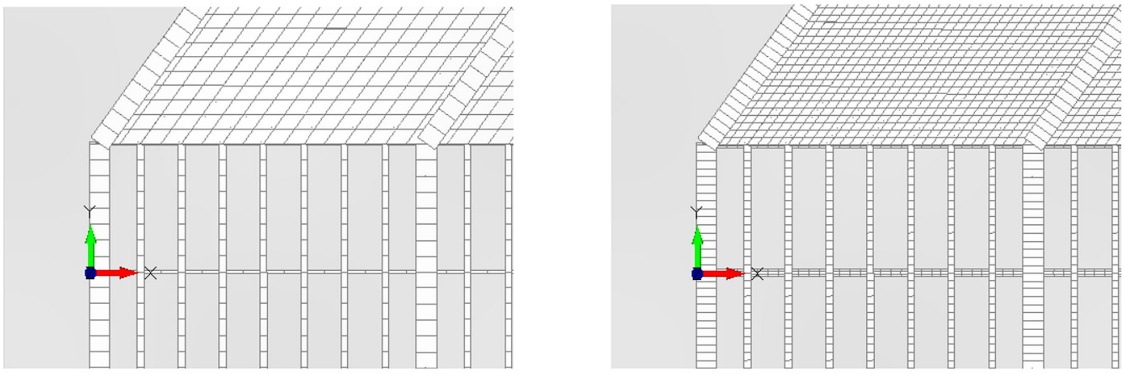

Fig. 7 Zoomed perspective of FE model of CRM with mesh densities corresponding to M1 (left) and M4 (right) models (without elements skins of the center wing box for visualization).

results from this mesh fineness exercise have been included here for the sake of completeness.

As a compromise, a local buckling analysis outside of MSC.NASTRAN is added, with the assumption that each buckling field is defined between two stiffeners and two ribs and is idealized as a simply supported flat plate under constant in-plane loading. The buckling analysis in this implementation solves an eigenvalue problem with shape functions for the bending displacement approximated as one-dimensional Lobatto polynomials. A similar analysis has been considered, for instance, in [79,80].

This hybrid approach considering a sufficiently tractable global model combined with a local subpanel buckling analysis, gives reasonably good results (denoted as M2+ in Table 6).

V. Optimization Parameters

A summary of the optimization objective and constraints included in the following optimization study is presented in Table 7. In addition to the lamination parameters and thickness for the shell elements, the stringers are modeled as T-stiffener beam elements where the height of the stiffener (h_{str}) is included as the design variable, with the flange width kept constant at 20 mm. The stringer is modeled with the same properties of an IM7 composite as in Table 3, corresponding to a hard laminate with an AML of −0.1, that is, a laminate with a large fraction of 0° plies with fiber along the stringer direction.

The wing is divided into 12 design fields in the spanwise direction, as shown with the colors in Fig. 5, with each design field having constant properties. The stringers in each region are also allocated the same property.

The requirement on ultimate load is introduced directly on the physical constraints through a safety factor of 1.5 over the limit loads. Buckling factors are subjected to a lower limit of 1.5. For the strain- and force-based failure modes, their respective failure indices are set with an upper limit of $1/1.5$, as shown in Table 7. In the case of the failure modes sandwich wrinkling, crimping, and dimpling, the failure index is calculated as the ratio between the element stress and failure stress, as shown in Table 1. For the stringer crippling, stringer strength, and core-shear failure modes, the allowable strain of the stringer (from Fig. 6) and the core shear strengths (S_{Lz} and S_{Wz} from Table 4) are used to arrive at the failure indices.

Table 7 Optimization summary

Optimization objective	min (structural weight)
Optimization constraints	
Feasibility	LP-space constraints
	Balance
	Standard angles (0°, 90°, ±45°)
	Angle fractions, $v_0, v_{90}, v_{\pm 45} > 0.1$
Physical	Buckling, $\lambda > 1.5$
	AML, $f_{\text{AML}} \leq 0.67$
	Stringer strength, $f_{\epsilon} \leq 0.67$
	Stringer crippling, $f_{\text{cripp}} \leq 0.67$
Physical (sandwich-specific)	Wrinkling, $f_{\text{wrink}} \leq 0.67$
	Crimping, $f_{\text{crimp}} \leq 0.67$
	Dimpling, $f_{\text{dimp}} \leq 0.67$
	Core-shear, $f_{\text{cshear}} \leq 0.67$
Design variables	
Monolithic design	$t, \xi^{A}_{1-4}, \xi^{D}_{1-4}; h_{str}$
Sandwich design	$t_f, t_c, \xi^{A}_{1-4}, \xi^{D}_{1-4}, \xi^{B_u}_{1-4}; h_{str}$

An in-house optimization framework in Python is used for the continuous optimization and is based on the finite element (FE) solver MSC.NASTRAN's design and sensitivity module SOL 200 and the Globally Convergent Method of Moving Asymptotes (GCMMA) [81,82]. The GCMMA has been used to solve structural optimization problems in earlier works as well [83].

Structural responses such as element strains, element forces, buckling factors, and their sensitivities are computed in MSC.NASTRAN. The element strains and forces are converted to various failure indices corresponding to the failure modes considered. The admissibility constraints for lamination parameters and their sensitivities are also calculated external to the FE solver within the optimization framework.

The assembled optimization problem, comprising an objective function, a list of constraints, their bounds, and sensitivities of the

Table 6 Comparison of optimization results between models having different mesh densities ("+" denotes optimization run including local subpanel buckling analysis as constraint; run-time from a standard workstation)

Model	Optimized mass (×1000 kg)	Buckling factor	Critical buckling factor (checked with M4 model)	Run time
M0	9.87	1.50, 1.51	1.02, 1.12	2 h
M1	10.40	1.50, 1.52	0.30, 0.40	8 h
M1+	10.81	1.50, 1.51	1.47, 1.22	8 h
M2	10.85	1.50, 1.52	1.00, 1.08	24 h
M2+	11.01	1.50, 1.50	1.50, 1.44	24 h
M4	10.97	1.50, 1.51	—, —	4 days

constraints with respect to the design variables, is fed to the GCMMA optimizer. The GCMMA algorithm casts the optimization problem as a series of approximated convex subproblems, which are solved iteratively. The subproblems are formulated using the responses and sensitivities of the objective and constraint functions of the original problem.

VI. Results and Discussion

The results from the optimization study comparing the wing designs using monolithic and sandwich composites are presented in this section.

A. Monolithic Versus Sandwich Composite Design

A comparison of the optimized weights of the primary structural components between the two designs is presented in Table 8. In this study, the structural components—skins, ribs, and spars—are assigned as monolithic and sandwich composites in the two runs. The stringers are always kept as monolithic T-stiffeners. While the ribs and spars include horizontal and vertical stiffeners, these are initially presized using handbook methods and are not considered in the optimization runs.

When considering the structural mass of the wing box, sandwich composites with the wing topology as-is offer potential weight savings of ∼12%. The largest weight savings arise from the upper skin and the ribs. The former can be expected given that the +2.5 g pull-up maneuver results in predominantly compression loads on the upper skin, thereby making it more active in buckling. In the case of the present CRM wing, several of the critical buckling modes are present in the ribs, thereby showing the largest weight savings as well.

Table 8 Comparison of mass of the wing structural components for baseline CRM wing

Component	Monolithic, kg	Sandwich, kg	ΔW, kg	ΔW, %
Upper skin	4,339.4	3,871.0	−468.4	−10.8
Lower skin	1,317.6	1,220.4	−97.2	−7.4
Ribs	1,875.0	1,343.7	−531.3	−28.3
Front spar	275.0	208.3	−66.7	−24.3
Rear spar	244.1	203.7	−40.4	−16.6
Midspar	155.1	47	−108.7	−69.7
Stringers (upper)	319.1	307.2	−11.9	−3.7
Stringers (lower)	500.0	461.2	−38.8	−7.8
Wing	10,729.0	9,366.2	−1362.8	−12.7

The spanwise thickness and constraints of the optimal designs are shown in Fig. 8 for the upper skin as an example. The strain failure and core shear (or force) failure indices adhere to an upper limit of 0.67, while buckling is enforced as a lower limit of 1.5. In the case of the strain and force failure indices, the critical failure index in the particular spanwise design field is characterized in the plot, while for buckling, the relative local amplitude of each mode together with its buckling factor is used to arrive at a spatial representation of the critical buckling factor. The thickness and failure index distribution on the upper skin contain the following distinct characteristics.

1) At the span-section between 10 and 20 m, the monolithic design is sized by strain or AML requirements. Consequently, in this region, the thickness of the facesheet is the same as that of the thickness of the monolithic laminate, with core thickness remaining at the minimum gauge set in the optimization.

2) At other segments of the wing, buckling appears to be driving the design. Consequently, the facesheet thickness in these regions is less than the monolithic thickness, with core material added in order to compensate for the bending stiffness required to tackle buckling.

3) The overall thickness of the sandwich design is greater than the monolithic counterpart. This can, however, be addressed by placing additional thickness constraints on the optimization to allow only a certain tolerance with respect to the thickness of the monolithic composite to account, for instance, for fuel volume.

4) For the considered aluminum honeycomb (Table 4), the high stiffness and strength properties result in the sandwich failure modes not being active, except for the core shear failure being critical in a small region of the wing.

A comparison of the volume fraction on the upper skin in the two optimized designs and the optimization history corresponding to the

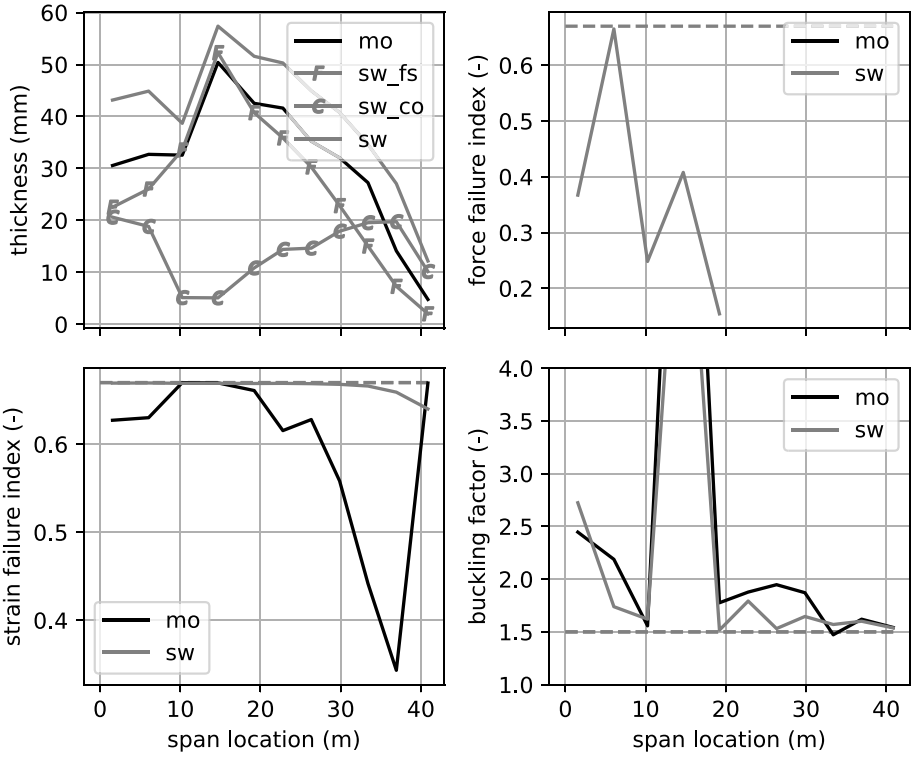

Fig. 8 Thickness comparison in the upper skin between optimized monolithic and sandwich design (mo, monolithic; sw, sandwich; sw_fs, sandwich facesheet; sw_co, sandwich core).

sandwich design is presented in Figs. 9 and 10 for the sake of completeness. The volume fraction of the 0° direction is comparatively higher for both designs, indicating the prominence of strain-based constraints. It is interesting to note that the volume fraction is higher in the case of the sandwich wing when compared to the monolithic design across nearly the entire wingspan. This can be explained by the fact that the monolithic wing requires a higher proportion of ±45° plies in order to tackle buckling. Given that the sandwich composite overcomes this in an easier manner by adding a core material, a larger portion of the laminate is available to be tailored along the 0° direction to meet strain requirements. The jumps in the objective and constraints in the optimization history are an artifact of the GCMMA algorithm, wherein a steepest descent is carried out in a first step followed by improving the conservativeness of the approximated response.

The spanwise thickness and constraints of the optimal designs are shown for the front spar and ribs for the sake of completeness in Figs. 11 and 12, respectively. In the case of the front spar, the facesheet thickness in the sandwich design in the midsection of the wing matches the thickness of the monolithic design, given that laminate strain is the dominant failure mode. At the root and tip sections where buckling drives the design, sandwich core material provides the necessary bending stiffness, leading to weight savings.

1. Aramid Core

A second option for the core material in the form of an aramid core is considered in the optimization study. The aramid core material is lighter in density and has the added advantage of better contact compatibility with carbon fiber materials, whereas contact with aluminum requires an additional treatment step to tackle galvanic corrosion. However, aramid as a core material has lower strength and stiffness when compared to its aluminum counterpart.

The result is that for a wing design with sandwich composites comprising an aramid core on all the primary structural members considered (skins, ribs, and spars), a feasible design is not obtained. This is on account of the sandwich failure modes of wrinkling, crimping, and core shear failure being simultaneously active in some sections of the wing, with countering requirements with respect to tackling them through adding or removing core material. This is particularly severe at the root segments of the wing with the highest loads.

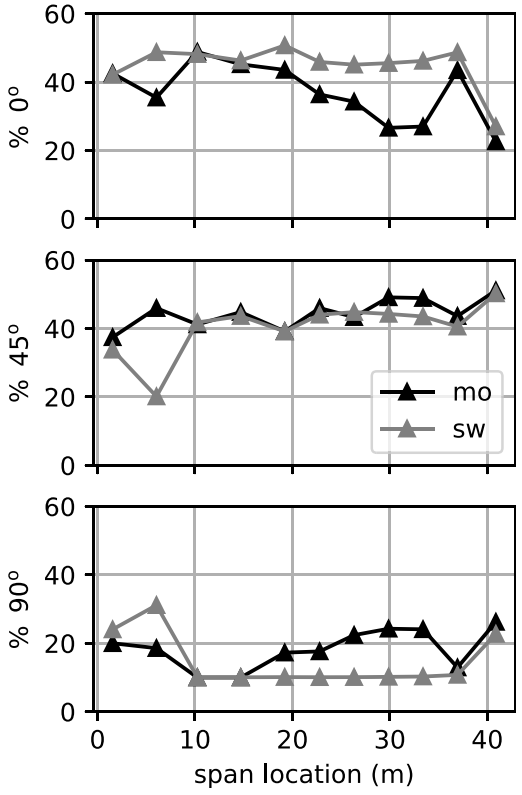

Fig. 9 Spanwise volume fractions in the upper skin for the optimized monolithic and sandwich wing design.

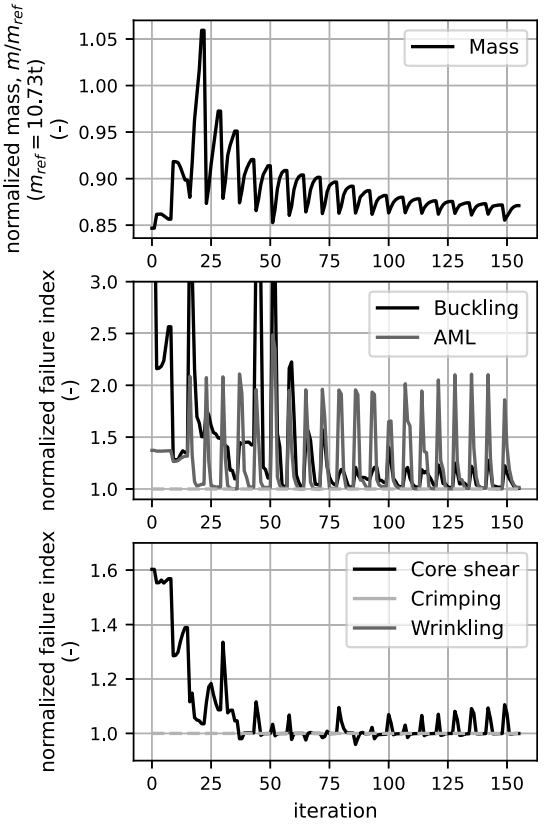

Fig. 10 Optimization history corresponding to the sandwich composite design in Sec. VI.A with aluminum honeycomb core (normalized failure index greater than 1.0 denotes constraint feasibility).

A study where different core materials are allocated to different sections of the wing, considering each of their advantages, might lead to more feasible designs but has not been considered in this work.

Extending the idea, using sandwich and monolithic composites in different regions of the wing, benefiting their strengths, would be done in reality in a more elaborate design study.

B. Variation in Wing Stringer Pitch

The skin-panel-level study on the CRM presented earlier [46] showed the possibility of increasing the stringer pitch in a sandwich design without impacting its weight. This would offer the added advantage of lower lifetime costs when accounting for manufacturing, inspection, and repairs. The stringer pitch is the distance between two stringers, 0.247 m in this configuration of the CRM wing.

A study was performed on the CRM wing, where the stringer pitch on the upper and lower skins was increased with respect to the baseline stringer pitch. This was done by removing alternative stringers in steps, up to the extreme case of a design without stringers. For each wing topology, a mass optimization was performed, and the results are summarized in Fig. 13. In the subsequent plots, the wing structural mass is normalized with respect to the monolithic design corresponding to the baseline version of the CRM wing (10,729 kg), which can be considered equivalent to today's state-of-the-art.

The trend in the weights of the sandwich design shows that the removal of stringers does not affect the optimized mass, because any reduction in stringer area is proportionally compensated for by an increase in skin thickness to counter strains, which are the dominant design driver. It is, however, surprising to note that the same trend is also observed in the monolithic design, where removal of stringers does not lead to an increase in the weight. The initial expectation

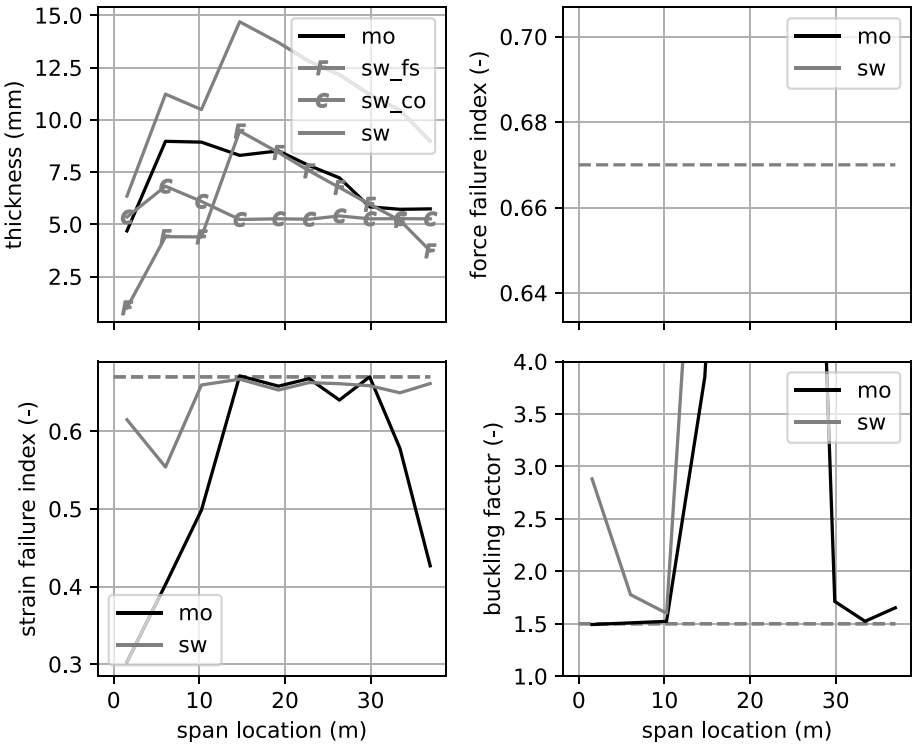

Fig. 11 Thickness comparison in the front spar between optimized monolithic and sandwich design (mo, monolithic; sw, sandwich; sw_fs, sandwich facesheet; sw_co, sandwich core).

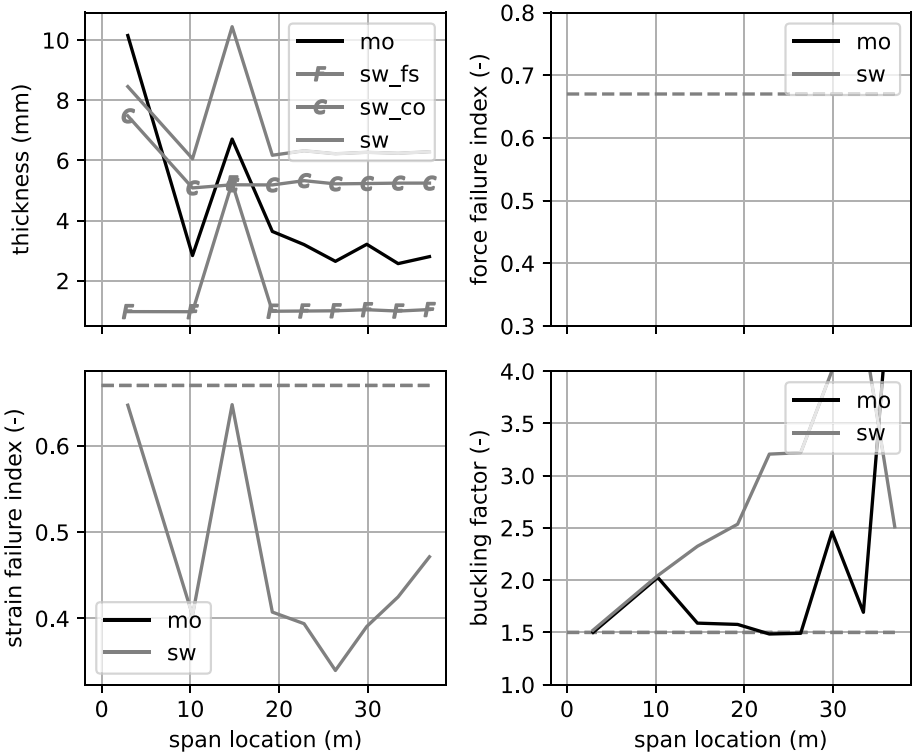

Fig. 12 Thickness comparison in the ribs between optimized monolithic and sandwich design (mo, monolithic; sw, sandwich; sw_fs, sandwich facesheet; sw_co, sandwich core).

would be that by removing stringers, the dimensions of the buckling field are increased and the bending stiffness of the stiffened panel is reduced, thereby making the design more susceptible to local buckling modes. As mentioned earlier, in the present CRM wing configuration, large portions of the wing are sized by strains. When stringers are removed, their equivalent in-plane stiffness is compensated by a proportional increase in skin thickness. With added skin thickness, the overall bending stiffness is still sufficient to address buckling, and in the present case, strains remain critical before buckling due to increased stringer pitch. This, however, changes in the case of modifying the rib pitch as discussed in the next section.

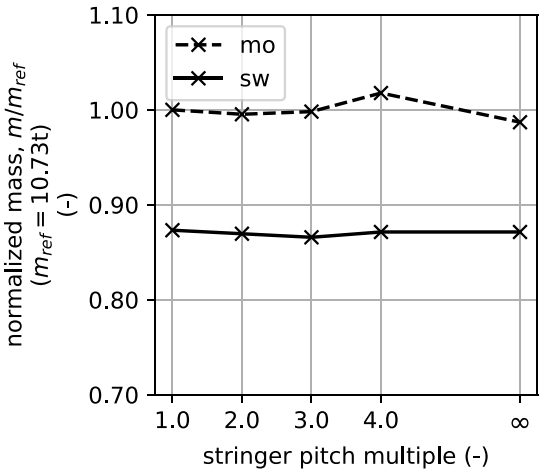

Fig. 13 Stringer pitch variation.

While structural weight is one important parameter driving topology characteristics such as stringer spacing, other requirements need to be considered as well. For instance, redundancy and damage tolerance, wherein damage to one stringer still allows the rest of the structure to be capable of carrying the required loads until the next repair; the cost of manufacturing and repairs; the type of loading in a given region; and the wing geometry, to name a few. An optimal choice for the stringer spacing would consider these relevant aspects as well.

C. Variation in Rib Pitch

The optimization study on the CRM wing was repeated with different rib pitches by removing subsequent ribs. The optimized weights for the monolithic and sandwich designs are summarized in Fig. 14. With an increase in rib pitch, the monolithic designs become heavier on account of the larger buckling fields, which drive buckling to become the driving failure mode. The sandwich design, on the other hand, benefits through a reduction in weight on account of the lesser number of ribs, while being able to address buckling through the addition of core material.

Given the influence of both stringer and rib pitch on the buckling behavior, it can be expected that an optimum topology from a weight perspective exists corresponding to the monolithic and sandwich designs. Another design parameter that can be varied is the stiffener pitch in the ribs and spars. These have not been varied in this work, and it can be expected that their variation would lead to a saving in weight for the sandwich design but lead to a more buckling-driven monolithic design.

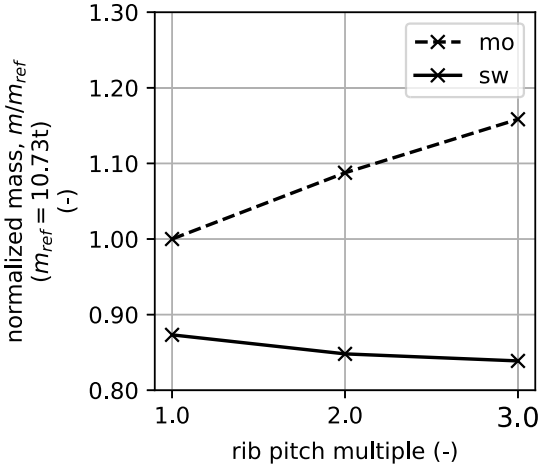

Fig. 14 Rib pitch variation.

D. Improvements in Facesheet Material

With advancements in materials beyond carbon fiber T300 and IM7, composite materials exhibiting improvements in failure strength can be expected. Under such scenarios, buckling is likely to size larger sections of the wing.

In order to simulate such a scenario, an optimization study was performed on the CRM wing by varying strain allowables from their open-hole (OHC, OHT) to unnotched (UNC, UNT) values. The OH values would represent today's class of materials, and the sweep toward UN would represent progressively improving materials offering larger strain allowables. As the material allowables are increased, the reduction in wing structural mass is limited for monolithic designs, as shown in Fig. 15, given that larger segments of the wing become sized by buckling. This, however, is not the case for the sandwich composite design, wherein the weight increase to curtail buckling is marginal and an increase in strain allowables affords large weight savings.

VII. Discussion

A. Further Aspects to be Considered in Sandwich Composite Design

In the present study, failure modes in the sandwich composite design are based on empirical and conservative methods presented in the CMH-17 [55]. This is by no means an exhaustive list of design criteria that need to be considered. Further aspects for the next detailed steps are mentioned here.

When sandwich composites with honeycomb cores are cured in a one-shot process, the facesheets in the manufactured structure exhibit imperfections in the form of waviness. The waviness results in an eccentricity in the loading, resulting in additional failure modes such as a crush and shear failure in the core and adhesive, as discussed in [84]. The loads at which these failure modes exist can be lower than the wrinkling loads as predicted in Eq. (4). One difficulty in modeling these failure modes is that the waviness is very dependent on the manufacturing process, and detailed micromechanic simulations of the composite manufacturing are needed to obtain realistic design-dependent values of the expected waviness.

A second aspect is the presence of rampdowns in a sandwich composite structure. Such rampdowns are primarily present at the junction between the skin and spars in case the sandwich design tapers to a monolithic laminate at the joints or when there is a variation in the core or facesheet thickness along the structure. The presence of a rampdown introduces out-of-plane stresses, causing crushing failure in the core, the adhesive to fail in tension, or additional stresses in the facesheet due to effective stress concentrations at the rampdown curvature. Analytical methods to predict the local stresses have been developed, for instance, in [85,86]. Failure indices or knockdowns in allowables can be included based on these stress models at the regions of the rampdowns in order to include their effects in the global optimization.

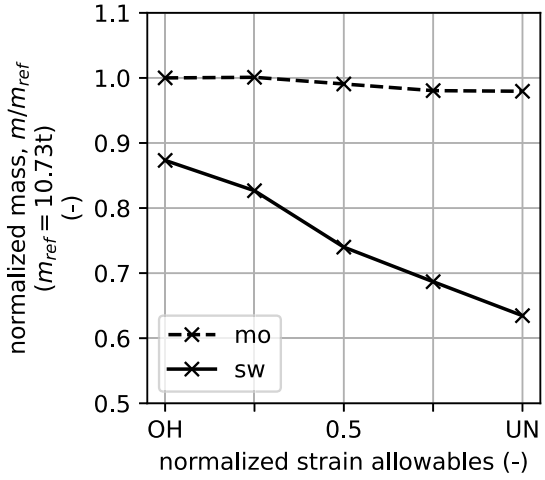

Fig. 15 Optimal wing-box mass considering different levels of strain allowables.

The mass of the sandwich components in the considered simulation models is composed of contributions from the facesheet and core. The adhesive that serves to hold the facesheet and core together and to transmit loads between them is not considered. Typical thicknesses of the adhesives that are present in literature have a thickness of ∼0.1–0.5 mm. Assuming the higher end of this thickness range results in a total adhesive weight of ∼70 kg for the two skins.

One of the advantages of sandwich composites discussed earlier in Sec. I is that for sections of the wing sized by minimum thickness requirements due to handling, sandwich composites offer a more efficient solution to monolithic composites. The thickness requirements that would also affect each sandwich facesheet if cured independently can be circumvented by cocuring the sandwich composite. This process involves simultaneously bonding and curing the individual facesheets and core and is commonly applied in the aerospace industry already. Cocuring is advantageous due to a typically higher bond strength and overall structural integrity. The downside of cocuring would include more complex tooling and precise control of process parameters to prevent core crushing, for example.

The present study is focused on the stiffness optimization step, and a stacking sequence retrieval is required in order to arrive at a manufacturable stacking sequence. This is seen as an independent problem where several solutions have already been studied extensively, for instance, in [15,65–67]. Typically, when going from lamination parameters to stacking sequence, an increase in weight is observed on account of simplifications made in the lamination parameter realm when it comes to the discrete nature of the thickness and ply angles as design variables.

The resulting mass increase from the above-mentioned aspects needs to be kept in mind when comparing weight benefits.

B. Performance Comparison and Dependence on Wing Model

The CRM wing is a heavily loaded wing on account of its large span. A different reference wing that shows dominant buckling-driven regions [15] could show significantly different savings in weight. Moreover, the initial topology that is considered in terms of stringer and rib pitch also plays a role in any weight comparison.

In the next step, wing designs with varying geometry, topology, and loading need to be studied in order to better understand the types of wings that are naturally suited to sandwich composite designs and those to monolithic ones.

VIII. Conclusions

This paper presents an optimization methodology and a study on the CRM wing, comparing structural weight performance between monolithic and sandwich composite designs. The methodology proposed builds on earlier works presented by the authors and aims to represent design studies with a level of fidelity suited to a preliminary stage of aircraft design.

The approach combines finite element analyses and conservative empirical relations to model failure mechanisms in sandwich composites, with the focus being on the optimization approach rather than detailed models of the failure modes.

The optimization studies on the CRM wing show that the sandwich composites can result in weight savings of ∼12% over today's state-of-the-art monolithic composites. This arises due to their efficiency in addressing buckling failure through the addition of core material. The studies also show that the topology of the wing in the form of the number of stringers and ribs is also an important design parameter to be varied without necessarily imposing weight penalties through the use of sandwich composites. This could potentially raise discussions on savings in manufacturing, maintenance, and inspection costs. Furthermore, with continuing improvement in material properties of carbon fiber, the use of sandwich composites can offer one possible solution of harnessing this potential advancement more efficiently than with monolithic designs.

In a next step, the optimization approach presented can be applied to wing configurations with different geometry, loading, and topology in order to better understand the types of wing structures where monolithic or sandwich composites show relative weight benefits and quantify them.

Acknowledgment

The authors would like to thank Prof. Christos Kassapoglou for his valuable insight and discussions during the course of this work.

References

[1] Fualdes, C., "Experience and Lessons Learned of a Composite Aircraft," *30th Congress of the International Council of the Aeronautical Sciences*, 2016.

[2] Kodiyalam, S., Nagendra, S., and DeStefano, J., "Composite Sandwich Structure Optimization with Application to Satellite Components," *AIAA Journal*, Vol. 34, No. 3, 1996, pp. 614–621. https://doi.org/10.2514/3.13112

[3] Herrmann, A. S., Zahlen, P. C., and Zuardy, I., "Sandwich Structures Technology in Commercial Aviation," *Sandwich Structures 7: Advancing with Sandwich Structures and Materials*, edited by O. Thomsen, E. Bozhevolnaya, and A. Lyckegaard, Springer-Verlag, Berlin, 2005, pp. 13–26. https://doi.org/10.1007/1-4020-3848-8_2

[4] Chen, J., Wang, Q., Shen, W. Z., Pang, X., Li, S., and Guo, X., "Structural Optimization Study of Composite Wind Turbine Blade," *Materials & Design*, Vol. 46, 2013, pp. 247–255. https://doi.org/10.1016/j.matdes.2012.10.036

[5] Barnes, R., and Morozov, E., "Structural Optimisation of Composite Wind Turbine Blade Structures with Variations of Internal Geometry Configuration," *Composite Structures*, Vol. 152, 2016, pp. 158–167. https://doi.org/10.1016/j.compstruct.2016.05.013

[6] Sjølund, J., Peeters, D., and Lund, E., "Discrete Material and Thickness Optimization of Sandwich Structures," *Composite Structures*, Vol. 217, 2019, pp. 75–88. https://doi.org/10.1016/j.compstruct.2019.03.003

[7] Kim, Y., and Park, J., "An Optimization of Composite Sandwich Structure with Passive Vibration Absorber for Vibration Suppression," *Journal of Sandwich Structures & Materials*, Vol. 23, No. 8, 2021, pp. 3717–3745. https://doi.org/10.1177/1099636220942913

[8] Castanie, B., Bouvet, C., and Ginot, M., "Review of Composite Sandwich Structure in Aeronautic Applications," *Composites Part C: Open Access*, Vol. 1, 2020, Paper 100004. https://doi.org/10.1016/j.jcomc.2020.100004

[9] van Vuure, A., Ivens, J., and Verpoest, I., "Mechanical Properties of Composite Panels Based On Woven Sandwich-Fabric Preforms," *Composites Part A: Applied Science and Manufacturing*, Vol. 31, No. 7, 2000, pp. 671–680. https://doi.org/10.1016/S1359-835X(00)00017-8

[10] Jakobsen, J., Bozhevolnaya, E., and Thomsen, O., "New Peel Stopper Concept for Sandwich Structures," *Composites Science and Technology*, Vol. 67, Nos. 15–16, 2007, pp. 3378–3385. https://doi.org/10.1016/j.compscitech.2007.03.033

[11] Fogarty, J. H., "Honeycomb Core and the Myths of Moisture Ingression," *Applied Composite Materials*, Vol. 17, No. 3, 2010, pp. 293–307. https://doi.org/10.1007/s10443-009-9121-7

[12] Das, M., Sahu, S., and Parhi, D., "Composite Materials and Their Damage Detection Using AI Techniques for Aerospace Application: A Brief Review," *Materials Today: Proceedings*, Vol. 44, 2021, pp. 955–960. https://doi.org/10.1016/j.matpr.2020.11.005

[13] Tewari, K., Pandit, M., Budarapu, P., and Natarajan, S., "Analysis of Sandwich Structures with Corrugated and Spiderweb-Inspired Cores for Aerospace Applications," *Thin-Walled Structures*, Vol. 180, 2022, Paper 109812. https://doi.org/10.1016/j.tws.2022.109812

[14] Stodieck, O., Cooper, J. E., Weaver, P. M., and Kealy, P., "Aeroelastic Tailoring of a Representative Wing Box Using Tow-Steered Composites," *AIAA Journal*, Vol. 55, No. 4, 2017, pp. 1425–1439. https://doi.org/10.2514/1.J055364

[15] Silva, G. H. C., do Prado, A. P., Cabral, P. H., De Breuker, R., and Dillinger, J. K. S., "Tailoring of a Composite Regional Jet Wing Using the Slice and Swap Method," *Journal of Aircraft*, Vol. 56, No. 3, 2019, pp. 990–1004. https://doi.org/10.2514/1.C035094

[16] Brooks, T. R., Martins, J. R., and Kennedy, G. J., "High-Fidelity Aerostructural Optimization of Tow-Steered Composite Wings," *Journal of Fluids and Structures*, Vol. 88, 2019, pp. 122–147. https://doi.org/10.1016/j.jfluidstructs.2019.04.005

[17] Wang, Z., Wan, Z., Groh, R. M., and Wang, X., "Aeroelastic and Local Buckling Optimisation of a Variable-Angle-Tow Composite Wing-Box Structure," *Composite Structures*, Vol. 258, 2021, Paper 113201. https://doi.org/10.1016/j.compstruct.2020.113201

[18] Chae, H. G., Newcomb, B. A., Gulgunje, P. V., Liu, Y., Gupta, K. K., Kamath, M. G., Lyons, K. M., Ghoshal, S., Pramanik, C., Giannuzzi, L., et al., "High Strength and High Modulus Carbon Fibers," *Carbon*, Vol. 93, 2015, pp. 81–87. https://doi.org/10.1016/j.carbon.2015.05.016

[19] Stiftinger, M., and Rammerstorfer, F., "Face Layer Wrinkling in Sandwich Shells–Theoretical and Experimental Investigations," *Thin-Walled Structures*, Vol. 29, Nos. 1–4, 1997, pp. 113–127. https://doi.org/10.1016/S0263-8231(97)00018-9

[20] Fagerberg, L., "Wrinkling and Compression Failure Transition in Sandwich Panels," *Journal of Sandwich Structures & Materials*, Vol. 6, No. 2, 2004, pp. 129–144. https://doi.org/10.1177/1099636204030475

[21] Fagerberg, L., and Zenkert, D., "Imperfection-Induced Wrinkling Material Failure in Sandwich Panels," *Journal of Sandwich Structures & Materials*, Vol. 7, No. 3, 2005, pp. 195–219. https://doi.org/10.1177/1099636205048526

[22] Carrera, E., "Theories and Finite Elements for Multilayered Plates and Shells: A Unified Compact Formulation with Numerical Assessment and Benchmarking," *Archives of Computational Methods in Engineering*, Vol. 10, No. 3, 2003, pp. 215–296. https://doi.org/10.1007/BF02736224

[23] Caliri, M. F., Ferreira, A. J., and Tita, V., "A Review on Plate and Shell Theories for Laminated and Sandwich Structures Highlighting the Finite Element Method," *Composite Structures*, Vol. 156, 2016, pp. 63–77. https://doi.org/10.1016/j.compstruct.2016.02.036

[24] Schmit, L. A., and Mehrinfar, M., "Multilevel Optimum Design of Structures with Fiber-Composite Stiffened-Panel Components," *AIAA Journal*, Vol. 20, No. 1, 1982, pp. 138–147. https://doi.org/10.2514/3.51060

[25] Miki, M., and Sugiyama, Y., "Optimum Design of Laminated Composite Plates Using Lamination Parameters," *32nd Structures, Structural Dynamics, and Materials Conference*, AIAA Paper 1991-971, 1991. https://doi.org/10.2514/6.1991-971

[26] Moh, J.-S., and Hwu, C., "Optimization for Buckling of Composite Sandwich Plates," *AIAA Journal*, Vol. 35, No. 5, 1997, pp. 863–868. https://doi.org/10.2514/2.7459

[27] Venter, G., and Sobieszczanski-Sobieski, J., "Multidisciplinary Optimization of a Transport Aircraft Wing Using Particle Swarm Optimization," *Structural and Multidisciplinary Optimization*, Vol. 26, Nos. 1–2, 2004, pp. 121–131. https://doi.org/10.1007/s00158-003-0318-3

[28] Lin, C.-C., and Lee, Y.-J., "Stacking Sequence Optimization of Laminated Composite Structures Using Genetic Algorithm with Local Improvement," *Composite Structures*, Vol. 63, Nos. 3–4, 2004, pp. 339–345. https://doi.org/10.1016/S0263-8223(03)00182-X

[29] Yuan, C., Bergsma, O., Koussios, S., Zu, L., and Beukers, A., "Optimization of Sandwich Composites Fuselages Under Flight Loads," *Applied Composite Materials*, Vol. 19, No. 1, 2012, pp. 47–64. https://doi.org/10.1007/s10443-010-9180-9

[30] Balabanov, V., Weckner, O., Epton, M., Mabson, G., Cregger, S., and Blom, A., "Optimal Design of a Composite Sandwich Structure Using Lamination Parameters," *53rd AIAA/ASME/ASCE/AHS/ASC Structures, Structural Dynamics and Materials Conference Astronautics*, AIAA Paper 2012-1520, 2012. https://doi.org/10.2514/6.2012-1520

[31] Lee, G.-C., Kweon, J.-H., and Choi, J.-H., "Optimization of Composite Sandwich Cylinders for Underwater Vehicle Application," *Composite Structures*, Vol. 96, 2013, pp. 691–697. https://doi.org/10.1016/j.compstruct.2012.08.055

[32] Weckner, O., and Balabanov, V., "Efficient Design of Shear-Deformable Hybrid Composite Structures," U.S. Patent 8,645,110, Feb. 2014.

[33] Jin, P., Song, B., Zhong, X., Yu, T., and Xu, F., "Aeroelastic Tailoring of Composite Sandwich Panel with Lamination Parameters," *Proceedings of the Institution of Mechanical Engineers, Part G: Journal of Aerospace Engineering*, Vol. 230, No. 1, 2016, pp. 105–117. https://doi.org/10.1177/0954410015587724

[34] Montemurro, M., Catapano, A., and Doroszewski, D., "A Multi-Scale Approach for the Simultaneous Shape and Material Optimisation of Sandwich Panels with Cellular Core," *Composites Part B: Engineering*, Vol. 91, 2016, pp. 458–472. https://doi.org/10.1016/j.compositesb.2016.01.030

[35] Coburn, B. H., and Weaver, P. M., "Buckling Analysis, Design and Optimisation of Variable-Stiffness Sandwich Panels," *International Journal of Solids and Structures*, Vol. 96, 2016, pp. 217–228. https://doi.org/10.1016/j.ijsolstr.2016.06.007

[36] Julien, C., Irisarri, F.-X., Bettebghor, D., Lavelle, F., and Mathis, K., "Optimisation of Sandwich Composite Structures for Space Applications," *JEC Composites Magazine*, Vol. 54, 2017, pp. 51–53.

[37] Fan, H.-T., Wang, H., and Chen, X.-H., "Optimization of Multi-Sandwich-Panel Composite Structures for Minimum Weight with Strength and Buckling Considerations," *Science and Engineering of Composite Materials*, Vol. 25, No. 2, 2018, pp. 229–241. https://doi.org/10.1515/secm-2015-0171

[38] Moors, G., Kassapoglou, C., de Almeida, S. F. M., and Ferreira, C. A. E., "Weight Trades in the Design of a Composite Wing Box: Effect of Various Design Choices," *CEAS Aeronautical Journal*, Vol. 10, No. 2, 2019, pp. 403–417. https://doi.org/10.1007/s13272-018-0321-4

[39] Silva, G. H. C., and Meddaikar, Y., "Lamination Parameters for Sandwich and Hybrid Material Composites," *AIAA Journal*, Vol. 58, No. 10, 2020, pp. 1–8. https://doi.org/10.2514/1.J059093

[40] Irisarri, F.-X., Julien, C., Bettebghor, D., Lavelle, F., Guerin, Y., and Mathis, K., "A General Optimization Strategy for Composite Sandwich Structures," *Structural and Multidisciplinary Optimization*, Vol. 63, No. 6, 2021, pp. 3027–3044. https://doi.org/10.1007/s00158-021-02849-8

[41] Löffelmann, F., "Discrete Material Optimization with Sandwich Failure Constraints," *Structural and Multidisciplinary Optimization*, Vol. 64, No. 4, 2021, pp. 2513–2523. https://doi.org/10.1007/s00158-021-03006-x

[42] Seyyedrahmani, F., Khandar Shahabad, P., Serhat, G., Bediz, B., and Basdogan, I., "Multi-Objective Optimization of Composite Sandwich Panels Using Lamination Parameters and Spectral Chebyshev Method," *Composite Structures*, Vol. 289, 2022, Paper 115417. https://doi.org/10.1016/j.compstruct.2022.115417

[43] Palm, T., Mahler, M., Shah, C., Rouse, M., Bush, H., Wu, C., and Small, W., "BMI Sandwich Wing Box Analysis and Test," *41st Structures, Structural Dynamics, and Materials Conference and Exhibit*, AIAA Paper 2000-1342, 2000. https://doi.org/10.2514/6.2000-1342

[44] Ilcewicz, L., Smith, P., Hanson, C., Walker, T., Metschan, S., Mabson, G., Wilden, K., Flynn, B., Scholz, D., and Polland, D., " Advanced Technology Composite Fuselage: Program Overview," NASA CR 4734, Langley Research Center, 1997.

[45] Scholz, D., Dost, E., Flynn, B., Ilcewicz, L., Nelson, K., Sawicki, A., Walker, T., and Lakes, R., "Advanced Technology Composite Fuselage-Materials and Processes," NASA CR 4731, Langley Research Center, 1997.

[46] Meddaikar, Y. M., Dillinger, J. K. S., Silva, G. H. C., and De Breuker, R., "Skin Panel Optimization of the Common Research Model Wing Using Sandwich Composites," *Journal of Aircraft*, Vol. 59, No. 2, 2022, pp. 386–399. https://doi.org/10.2514/1.C036551

[47] Feraboli, P., "Composite Materials Strength Determination Within the Current Certification Methodology for Aircraft Structures," *Journal of Aircraft*, Vol. 46, No. 4, 2009, pp. 1365–1374. https://doi.org/10.2514/1.41286

[48] Vassberg, J. C., DeHaan, M. A., Rivers, M. S., and Wahls, R. A., "Retrospective on the Common Research Model for Computational Fluid Dynamics Validation Studies," *Journal of Aircraft*, Vol. 55, No. 4, 2018, pp. 1325–1337. https://doi.org/10.2514/1.C034906

[49] Klimmek, T., "Parametric Set-Up of a Structural Model for FERMAT Configuration for Aeroelastic and Loads Analysis," *Journal of Aeroelasticity and Structural Dynamics*, Vol. 2, 2014, pp. 31–49. https://doi.org/10.3293/asdj.2014.27-10.3293/asdj.2014.27

[50] Liu, Q., Jrad, M., Mulani, S. B., and Kapania, R. K., "Global/Local Optimization of Aircraft Wing Using Parallel Processing," *AIAA Journal*, Vol. 54, No. 11, 2016, pp. 3338–3348. https://doi.org/10.2514/1.J054499

[51] Stanford, B. K., "Aeroelastic Wingbox Stiffener Topology Optimization," *Journal of Aircraft*, Vol. 55, No. 3, 2018, pp. 1244–1251. https://doi.org/10.2514/1.C034653

[52] De, S., Jrad, M., and Kapania, R. K., "Structural Optimization of Internal Structure of Aircraft Wings with Curvilinear Spars and Ribs," *Journal of Aircraft*, Vol. 56, No. 2, 2019, pp. 707–718. https://doi.org/10.2514/1.C034818

[53] Brooks, T. R., Martins, J. R. R. A., and Kennedy, G. J., "Aerostructural Tradeoffs for Tow-Steered Composite Wings," *Journal of Aircraft*, Vol. 57, No. 5, 2020, pp. 787–799. https://doi.org/10.2514/1.C035699

[54] Wang, Z., Peeters, D., and De Breuker, R., "An Aeroelastic Optimisation Framework for Manufacturable Variable Stiffness Composite Wings Including Critical Gust Loads," *Structural and Multidisciplinary Optimization*, Vol. 65, No. 10, 2022, p. 290. https://doi.org/10.1007/s00158-022-03375-x

[55] "Design and Analysis of Sandwich Structures," *Composite Materials Handbook – 17*, Vol. 6, SAE International, Wichita, KS, 2017, Chap.4, pp. 1–228.

[56] Kassapoglou, C., *Design and Analysis of Composite Structures: With Applications to Aerospace Structures*, Wiley, Oxford, 2013, pp. 199, 270–275. https://doi.org/10.1002/9781118536933

[57] Hoff, N. J., and Mautner, S. E., "The Buckling of Sandwich-Type Panels," *Journal of the Aeronautical Sciences*, Vol. 12, No. 3, 1945, pp. 285–297. https://doi.org/10.2514/8.11246

[58] Zenkert, D., and Industrifond, N., *The Handbook of Sandwich Construction*, North European Engineering and Science Conference Series, Engineering Materials Advisory Services Ltd. (EMAS), Cradley Heath, West Midlands, 1997.

[59] Herencia, J. E., Weaver, P. M., and Friswell, M. I., "Optimization of Long Anisotropic Laminated Fiber Composite Panels with T-Shaped Stiffeners," *AIAA Journal*, Vol. 45, No. 10, 2007, pp. 2497–2509. https://doi.org/10.2514/1.26321

[60] Herencia, J. E., Haftka, R. T., Weaver, P. M., and Friswell, M. I., "Lay-Up Optimization of Composite Stiffened Panels Using Linear Approximations in Lamination Space," *AIAA Journal*, Vol. 46, No. 9, 2008, pp. 2387–2391. https://doi.org/10.2514/1.36189

[61] IJsselmuiden, S. T., Abdalla, M. M., Seresta, O., and Gürdal, Z., "Multi-Step Blended Stacking Sequence Design of Panel Assemblies with Buckling Constraints," *Composites Part B: Engineering*, Vol. 40, No. 4, 2009, pp. 329–336. https://doi.org/10.1016/j.compositesb.2008.12.002

[62] Irisarri, F.-X., Abdalla, M. M., and Gürdal, Z., "Improved Shepard's Method for the Optimization of Composite Structures," *AIAA Journal*, Vol. 49, No. 12, 2011, pp. 2726–2736. https://doi.org/10.2514/1.J051109

[63] Liu, D., and Toropov, V. V., "A Lamination Parameter-Based Strategy for Solving an Integer-Continuous Problem Arising in Composite Optimization," *Computers & Structures*, Vol. 128, 2013, pp. 170–174. https://doi.org/10.1016/j.compstruc.2013.06.003

[64] Liu, D., Toropov, V. V., Barton, D. C., and Querin, O. M., "Weight and Mechanical Performance Optimization of Blended Composite Wing Panels Using Lamination Parameters," *Structural and Multidisciplinary Optimization*, Vol. 52, No. 3, 2015, pp. 549–562. https://doi.org/10.1007/s00158-015-1244-x

[65] Meddaikar, Y. M., Irisarri, F.-X., and Abdalla, M. M., "Laminate Optimization of Blended Composite Structures Using a Modified Shepard's Method and Stacking Sequence Tables," *Structural and Multidisciplinary Optimization*, Vol. 55, No. 2, 2017, pp. 535–546. https://doi.org/10.1007/s00158-016-1508-0

[66] Autio, M., "Determining the Real Lay-up of a Laminate Corresponding to Optimal Lamination Parameters by Genetic Search," *Structural and Multidisciplinary Optimization*, Vol. 20, No. 4, 2000, pp. 301–310. https://doi.org/10.1007/s001580050160

[67] Irisarri, F.-X., Lasseigne, A., Leroy, F.-H., and Le Riche, R., "Optimal Design of Laminated Composite Structures with Ply Drops Using Stacking Sequence Tables," *Composite Structures*, Vol. 107, 2014, pp. 559–569. https://doi.org/10.1016/j.compstruct.2013.08.030

[68] Tsai, S. W., and Hahn, H. T., *Introduction to Composite Materials*, 2nd ed., Routledge, England, U.K., 2018, pp. 232–239. https://doi.org/10.1201/9780203750148

[69] Tsai, S. W., and Pagano, N. J., "Invariant Properties of Composite Materials," Air Force Materials Lab. AFML-TR-67-349, Wright-Patternson AFB Ohio, 1968.

[70] Kameyama, M., and Fukunaga, H., "Optimum Design of Composite Plate Wings for Aeroelastic Characteristics Using Lamination Parameters," *Computers & Structures*, Vol. 85, Nos. 3–4, 2007, pp. 213–224. https://doi.org/10.1016/j.compstruc.2006.08.051

[71] Diaconu, C., Sato, M., and Sekine, H., "Layup Optimization of Symmetrically Laminated Thick Plates for Fundamental Frequencies Using Lamination Parameters," *Structural and Multidisciplinary Optimization*, Vol. 24, No. 4, 2002, pp. 302–311. https://doi.org/10.1007/s00158-002-0241-z

[72] Diaconu, C. G., and Sekine, H., "Layup Optimization for Buckling of Laminated Composite Shells with Restricted Layer Angles," *AIAA Journal*, Vol. 42, No. 10, 2004, pp. 2153–2163. https://doi.org/10.2514/1.931

[73] Setoodeh, S., Abdalla, M., and Gürdal, Z., "Approximate Feasible Regions for Lamination Parameters," *11th AIAA/ISSMO Multidisciplinary Analysis and Optimization Conference*, AIAA Paper 2006-6973, 2006. https://doi.org/10.2514/6.2006-6973

[74] Bloomfield, M., Diaconu, C., and Weaver, P., "On Feasible Regions of Lamination Parameters for Lay-Up Optimization of Laminated Composites," *Royal Society A: Mathematical, Physical and Engineering Sciences*, Vol. 465, No. 2104, 2009, pp. 1123–1143. https://doi.org/10.1098/rspa.2008.0380

[75] Macquart, T., Bordogna, M. T., Lancelot, P., and De Breuker, R., "Derivation and Application of Blending Constraints in Lamination Parameter Space for Composite Optimisation," *Composite Structures*, Vol. 135, 2016, pp. 224–235. https://doi.org/10.1016/j.compstruct.2015.09.016

[76] Marlett, K., "Hexcel 8552 IM7 Unidirectional Prepreg 190 gsm & 35% RC Qualification Material Property Data Report," TR CAM-RP-2009-015 Rev A, National Inst. for Aviation Research, Wichita, KS, April 2011, pp. 33–61.

[77] Hexcel, "Honeycomb Sandwich Design Technology–Hexcel," 2000, https://www.hexcel.com/user_area/content_media/raw/Honeycomb_Sandwich_Design_Technology.pdf.

[78] Nastran, M. S. C., *Quick Reference Guide*, MSC Software Corp, Newport Beach, CA, 2017, p. 142.

[79] IJsselmuiden, S. T., Abdalla, M. M., and Gürdal, Z., "Optimization of Variable-Stiffness Panels for Maximum Buckling Load Using Lamination Parameters," *AIAA Journal*, Vol. 48, No. 1, 2010, pp. 134–143. https://doi.org/10.2514/1.42490

[80] Dillinger, J. K. S., Klimmek, T., Abdalla, M. M., and Gürdal, Z., "Stiffness Optimization of Composite Wings with Aeroelastic Constraints," *Journal of Aircraft*, Vol. 50, No. 4, 2013, pp. 1159–1168. https://doi.org/10.2514/1.C032084

[81] Svanberg, K., "The Method of Moving Asymptotes–A New Method for Structural Optimization," *International Journal for Numerical Methods in Engineering*, Vol. 24, No. 2, 1987, pp. 359–373. https://doi.org/10.1002/nme.1620240207

[82] Svanberg, K., "MMA and GCMMA, Versions Sept. 2007," *Optimization and Systems Theory*, Vol. 104, KTH Stockholm, Sweden, 2007, pp. 3–8.

[83] Wu, Z., Raju, G., and Weaver, P. M., "Framework for the Buckling Optimization of Variable-Angle Tow Composite Plates," *AIAA Journal*, Vol. 53, No. 12, 2015, pp. 3788–3804. https://doi.org/10.2514/1.J054029

[84] Kassapoglou, C., Chou, J., and Fantle, S., "Wrinkling of Composite Sandwich Structures Under Compression," *Composites Technology and Research*, Vol. 17, No. 4, 1995, pp. 308–316.

[85] Kassapoglou, C., "Stress Determination and Core Failure Analysis in Sandwich Rampdown Structures Under Bending Loads," *Key Engineering Materials*, Vol. 120, 1996, pp. 307–328.

[86] Paris, I., Hojjati, M., Chen, J., and Octeau, M., "Characterization of Composites Sandwich Ramp Failure Under Tensile Loading," *17th International Conference on Composite Material*, 2009.

J. Yang
Associate Editor